Electronic supplementary materials *Mendeleev Commun.*, 2018, **28**, 490–492

The relationship between the crystal structure and optical properties for isomeric aminopyridinium iodobismuthates

Petr A. Buikin, Andrey B. Ilyukhin, Alexander E. Baranchikov, Khursand E. Yorov and Vitalii Yu. Kotov

Methods and Materials

Synthesis of compound 1. The solution of 2-aminopyridine (0.5 g, 5.3 mmol, Acros, 99+%) and KI (2.57 g, 15.5 mmol, Reachim, A.C.S.) dissolved in a minimal amount of deionized water was added to the reaction mixture containing KI (5.14 g, 31 mmol), $Bi(NO_3)_3 \cdot 5H_2O$ (1.14 g, 2.35 mmol, Reachim, A.C.S.), and water (10 ml). The precipitated red powder immediately changed its color to the deep red one upon addition of H_2SO_4 (several drops). The pure phase of product **1** was isolated by filtration under vacuum and washing with ethanol. Yield: 1.359 g (71.2%). The Bi/I atomic ratio was 1 : 3.96±0.10 according to the EDX (Table S4). Single-crystal X-Ray data were collected on a crystal selected from the obtained product. The single-phase nature of compound **1** was confirmed by the XRD method [Figure S10(*a*)]. Details of the Rietveld refinement: space group is *P*bcn, a = 11.9893(3) Å, b = 15.2380(3) Å, c = 7.7532(2) Å, R_{exp}: 6.52%, R_{wp}: 7.72%, R_p: 6.04%, GOF: 1.18.

Synthesis of compound 2. The solution of 3-aminopyridine (0.5 g, 5.3 mmol, Acros, 99%) and KI (7.79 g, 47 mmol) dissolved in a minimal amount of deionized water was added to the reaction mixture containing KI (15.58 g, 93.9 mmol), $Bi(NO_3)_3 \cdot 5H_2O$ (2.30 g, 4.74 mmol), and water (20 ml). The precipitated orange powder immediately changed its color to the red one upon addition of H_2SO_4 (several drops). Compound **2** was isolated by filtration under vacuum and washing with ethanol. Yield: 2.547 g (66.1%). According to the EDX data (Table S5) for single crystals, the Bi/I atomic ratio was 1 : 4.09±0.11 while the overview was 1 : 4.44. Single-crystal X-Ray data were obtained for a crystal selected from the obtained

product. According to the XRD data [Figure S8(*b*)], compound **2** was not a single-phase one. An additional peak at $2\Theta = 7.2^{o}$ indicated the presence of an unidentified impurity. The unambiguous attribution of only the one peak to the admixture can be explained by the high degree of texturing of the impurity and the coincidence of a number of peaks of the major phase and impurity. This assumption was also indirectly confirmed by the positive ejections of a number of peaks on the difference curve [see Figure S8(*b*)]. Details of the Rietveld refinement: $P2_1/c$, a = 13.0939(6) Å, b = 14.1992(6) Å, c = 7.7396(3) Å, R_{exp}: 6.64%, R_{wp}: 11.39%, R_p: 8.95%, GOF: 1.72. All our attempts to purify this compound by recrystallization were unsuccessful.

Synthesis of compound 3. The solution of 4-aminopyridine (0.5 g, 5.3 mmol, Acros, 98%) and KI (9.03 g, 54.4 mmol) dissolved in a minimal amount of deionised water was added to the reaction mixture containing KI (18.06 g, 109 mmol), $Bi(NO_3)_3 \cdot 5H_2O$ (2.58 g, 5.32 mmol), and water (20 ml). The precipitated red powder immediately changed its color to the deep red one upon addition of H_2SO_4 (several drops). The pure phase of product **3** was isolated by filtration under vacuum and washing with ethanol. Yield: 3.446 g (79.8%). The Bi/I atomic ratio was 1 : 4.08±0.09 according to the EDX (Table S6). Single-crystal X-Ray data were obtained for a crystal selected from the obtained product. The single-phase nature of compound **3** was confirmed by the XRD method [Figure S8(*c*)]. Details of the Rietveld refinement: space group was *P*bcn, a = 12.3184(4) Å, b = 14.9411(3) Å, c = 7.7231(2) Å, R_{exp}: 6.30%, R_{wp}: 7.52%, R_p: 5.86%, GOF: 1.19.

X-Ray powder diffraction analysis was carried out on a Bruker D8 ADVANCE X-Ray diffractometer (CuKα, Ni-filter, LYNXEYE detector, reflection geometry). Full-profile X-ray analysis of patterns of crystalline substances was performed using TOPAS 4.2 software.[S1]

The chemical compositions of compounds were analyzed by energy-dispersive X-ray spectroscopy (EDX) using a Carl Zeiss NVision 40 scanning electron microscope equipped with Oxford Instruments X-Max detector at 20kV accelerating voltage. Carbon scotch tape was used as a support during the EDX measurements.

S1. A. A. Caelho, TOPAS-Academic, Version 4.2, Caelho software, Brisbane, Australian, 2009.

Table S1 Bond lengths [Å] for **1–4**.

1	
Bi(1)–I(2)	2.9415(4)
Bi(1)–I(1)	3.0780(3)
Bi(1)–I(1)$^{\#1}$	3.2502(4)

Symmetry transformations used to generate equivalent atoms:
$^{\#1}$ -x,-y,-z+2

2	
Bi(1)–I(2)	2.9064(5)
Bi(1)–I(4)	2.9143(5)
Bi(1)–I(1)	3.0931(5)
Bi(1)–I(3)	3.1059(5)
Bi(1)–I(1)$^{\#1}$	3.2526(5)
Bi(1)–I(3)$^{\#2}$	3.3106(5)

Symmetry transformations used to generate equivalent atoms:
$^{\#1}$ -x+1,-y,-z+1 $^{\#2}$ -x+2,-y,-z+1

3	
Bi(1)–I(2)	2.9566(3)
Bi(1)–I(1)	3.0724(3)
Bi(1)–I(1)$^{\#1}$	3.1916(3)

Symmetry transformations used to generate equivalent atoms:
$^{\#1}$ -x,-y,-z+1

4	
I(1)–I(2)	2.7973(8)
I(2)–I(3)	3.1068(8)
I(3)–I(4)	3.0195(8)
I(4)–I(5)	2.8405(8)

Table S2 Hydrogen bonds for **1**–**4** [Å and °].

D–H···A	*d*(D-H)	*d*(H···A)	*d*(D···A)	∠(DHA)
		1		
N(2)–H(2C)···I(2)	0.88	2.96	3.71(4)	144
N(2)–H(2C)···I(2)$^{\#1}$	0.88	3.35	3.90(2)	122
N(2)–H(2B)···I(2)$^{\#2}$	0.88	2.90	3.74(3)	161
N(1)–H(1A)···I(1)$^{\#3}$	0.88	3.09	3.759(16)	134
N(1)–H(1A)···I(2)$^{\#3}$	0.88	3.27	3.838(17)	125
C(2)–H(2A)···I(1)$^{\#1}$	0.95	2.99	3.876(14)	156
C(4)–H(4A)···I(2)$^{\#4}$	0.95	3.24	3.983(11)	137
C(5)–H(5A)···I(1)$^{\#3}$	0.95	3.28	3.877(10)	122

Symmetry transformations used to generate equivalent atoms:
$^{\#\#1}$ -x+1/2,-y+1/2,z-1/2 $^{\#\#2}$ -x,y,-z+1/2 $^{\#\#3}$ x-1/2,-y+1/2,-z+1 $^{\#\#4}$ -x,-y+1,-z+1

		2		
N(1)–H(1A)···I(2)$^{\#1}$	0.88	3.29	3.97(3)	136
N(1)–H(1A)···I(4)$^{\#1}$	0.88	3.00	3.71(3)	138
C(1)–H(1B)···I(3)$^{\#2}$	0.95	3.28	4.17(3)	158
C(1)–H(1B)···I(4)$^{\#1}$	0.95	3.27	3.85(3)	121
C(4)–H(4A)···I(2)$^{\#3}$	0.95	2.99	3.93(3)	170
C(5)–H(5A)···I(1)$^{\#4}$	0.95	3.09	4.01(3)	162
N(2)–H(2B)···I(3)$^{\#5}$	0.88	3.14	4.01(3)	172
N(2)–H(2A)···I(4)$^{\#6}$	0.88	3.09	3.602(18)	119
N(1B)–H(1BA)···I(4)$^{\#1}$	0.88	2.78	3.51(2)	141
C(1B)–H(1BB)···I(3)$^{\#2}$	0.95	3.21	4.13(2)	163
C(3B)–H(3BA)···I(1)	0.95	3.39	4.28(2)	156
C(4B)–H(4BA)···I(2)$^{\#3}$	0.95	3.03	3.98(2)	172
C(5B)–H(5BA)···I(1)$^{\#4}$	0.95	3.13	3.98(2)	150
C(5B)–H(5BA)···I(2)$^{\#1}$	0.95	3.18	3.84(2)	128
N(2B)–H(2BB)···I(3)$^{\#5}$	0.88	3.24	4.08(3)	160
N(2B)–H(2BA)···I(4)$^{\#6}$	0.88	3.21	3.76(2)	122
N(1C)–H(1CA)···I(1)	0.88	3.20	3.86(2)	134
N(1C)–H(1CA)···I(2)$^{\#3}$	0.88	2.97	3.730(18)	146

C(1C)–H(1CB)···I(1)	0.95	3.24	3.897(19)	128
C(3C)–H(3CA)···I(4)[#1]	0.95	3.29	4.08(2)	142
C(4C)–H(4CA)···I(2)[#1]	0.95	3.12	4.02(2)	160
C(5C)–H(5CA)···I(1)[#4]	0.95	3.06	3.97(2)	162
N(2C)–H(2CB)···I(3)[#2]	0.88	3.20	4.07(3)	172

_

Symmetry transformations used to generate equivalent atoms:

[##1] -x+1,-y+1,-z+1 [#2] -x+1,y+1/2,-z+1/2 [#3] x,-y+1/2,z+1/2 [#4] -x+1,y+1/2,-z+3/2 [#5] x-1,y,z [#6] x-1,-y+1/2,z-1/2

3

N(1)–H(1B)···I(2)[#1]	0.88	3.06	3.714(4)	133
N(1)–H(1B)···I(2)[#2]	0.88	3.06	3.714(4)	133
N(2)–H(2B)···I(2)[#3]	0.90	2.96	3.727(2)	144

_

Symmetry transformations used to generate equivalent atoms:

[##1] -x,-y+1,-z+1 [##2] x,-y+1,z-1/2 [##3] x,y,z-1

4

N(1)–H(1A)···I(4)[#1]	0.88	3.15	3.940(18)	150
N(1)–H(1A)···I(5)[#2]	0.88	3.29	3.844(19)	123
N(1)–H(1A)···I(5)[#1]	0.88	3.31	3.874(17)	124
C(4)–H(4A)···I(2)[#2]	0.95	3.13	4.00(3)	152
C(5)–H(5A)···I(3)[#3]	0.95	3.09	3.80(2)	133
C(5)–H(5A)···I(4)[#2]	0.95	3.23	3.93(2)	132
N(2)–H(2B)···I(1)[#2]	0.88	3.00	3.742(14)	144
N(2)–H(2C)···I(5)[#4]	0.88	3.16	3.873(14)	140
N(2)–H(2C)···I(5)[#5]	0.88	2.97	3.642(14)	135

_

Symmetry transformations used to generate equivalent atoms:

[#1] -x+1,y-1/2,-z+1/2 [#2] -x+1,-y+1,-z [#3] x+1,y,z [#4] -x,-y+1,-z [#5] -x,y-1/2,-z+1/2

Table S3 Crystal structure parameters similar to that of compound **2.**

Refcode[26]	space group	*a*/Å	*b*/Å	*c*/, Å	*β*/°	cell volume/Å^3
AYENEZ[17]	$P2_1/c$	7.470	13.177	13.910	95.11	1363.7
AYENOJ[17]	$P2_1/c$	7.649	13.153	13.703	96.48	1369.8
AYEPAX[17]	$P2_1/c$	7.797	13.087	13.551	97.93	1369.5
NACNOX[27]	$P2_1/c$	7.473	13.344	12.470	91.99	1242.9
PAQLEB[25]	$P2_1/c$	7.762	14.041	13.196	92.96	1436.2
POVYUU[11]	$P2_1/c$	7.476	13.194	13.916	95.22	1367.0
RAZMEN[28]	$P2_1/c$	7.444	13.095	13.794	95.16	1339.1
2	$P2_1/c$	7.666	14.110	12.926	93.28	1395.9

Table S4 Results of EDX analysis for **1.**

Spectrum	C (at%)	I (at%)	Bi (at%)	I/Bi
Spectrum 1	64.81	28.30	6.89	4.11
Spectrum 2	75.73	19.34	4.92	3.93
Spectrum 3	74.30	20.40	5.31	3.84

Table S5 Results of EDX analysis for **2.**

Spectrum	C (at%)	I (at%)	Bi (at%)	I/Bi
Spectrum 1	74.73	20.14	5.13	3.93
Spectrum 2	73.51	21.39	5.10	4.19
Spectrum 3	66.21	27.24	6.55	4.16
Spectrum 4 (overview)	67.30	26.69	6.01	4.44

Table S6 Results of EDX analysis for **3.**

Spectrum	C (at%)	I (at%)	Bi (at%)	I/Bi
Spectrum 1	67.72	26.06	6.21	4.20
Spectrum 2	73.99	20.74	5.26	3.94
Spectrum 3	86.62	10.75	2.63	4.09

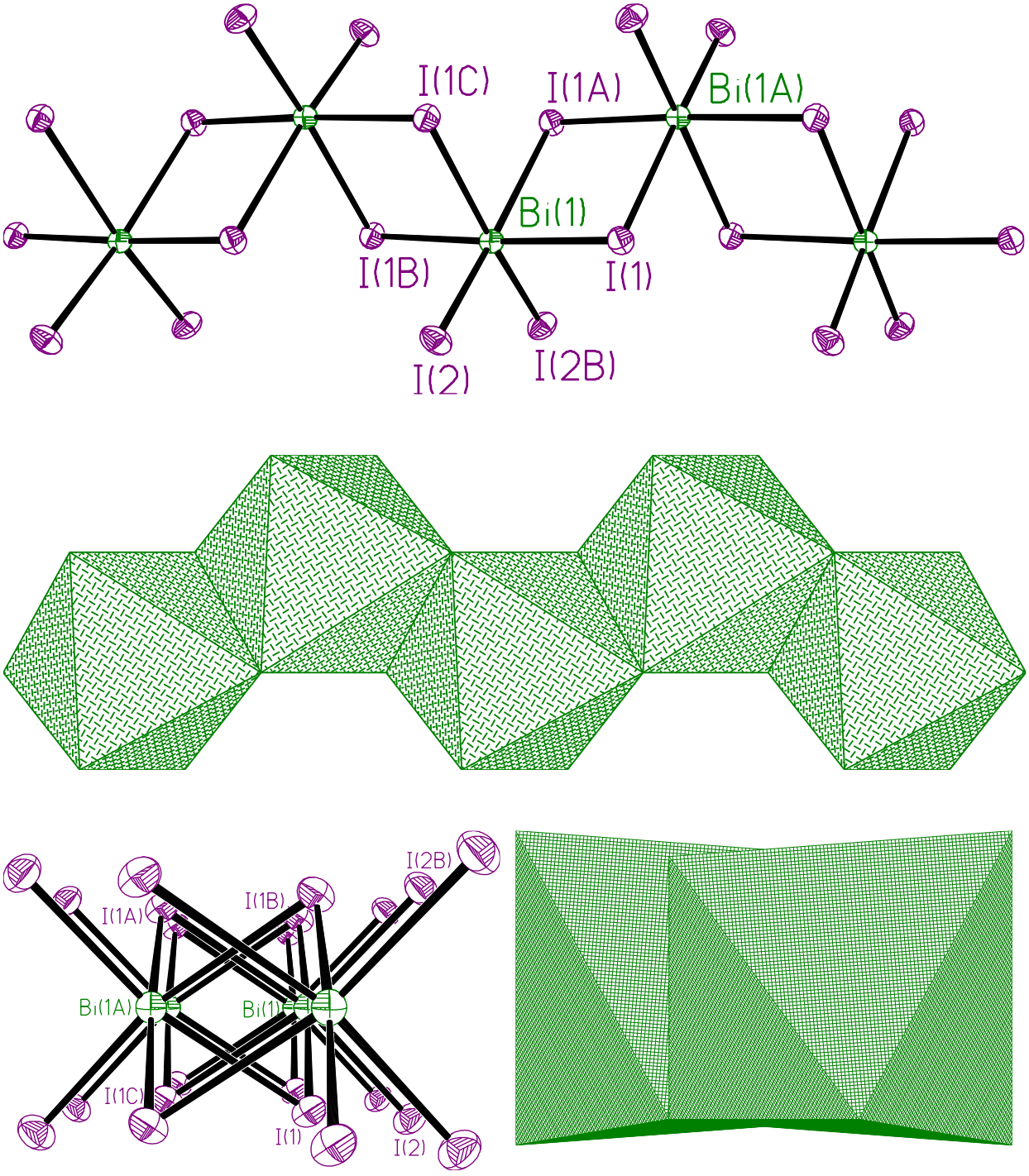

Figure S1 Projections of 1D chains in **1** (the thermal ellipsoids are shown at 50% probability level).

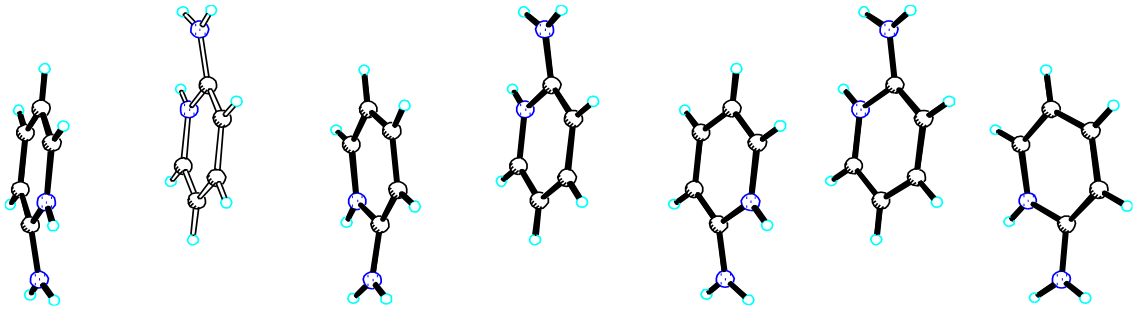

Figure S2 The spatial location of the 2-NH_2PyH^+ cations in **1**.

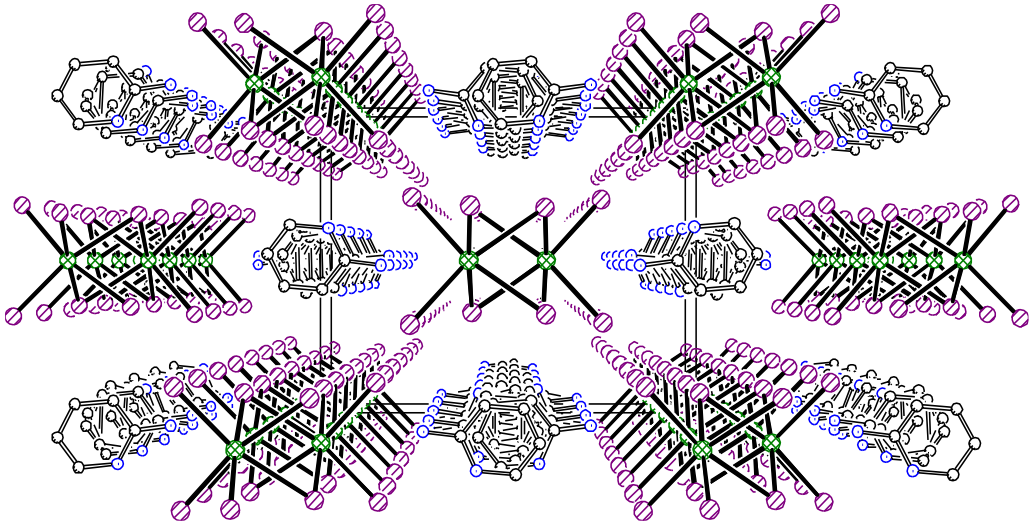

Figure S3 Projection of the structure of **1** along the *c* axis.

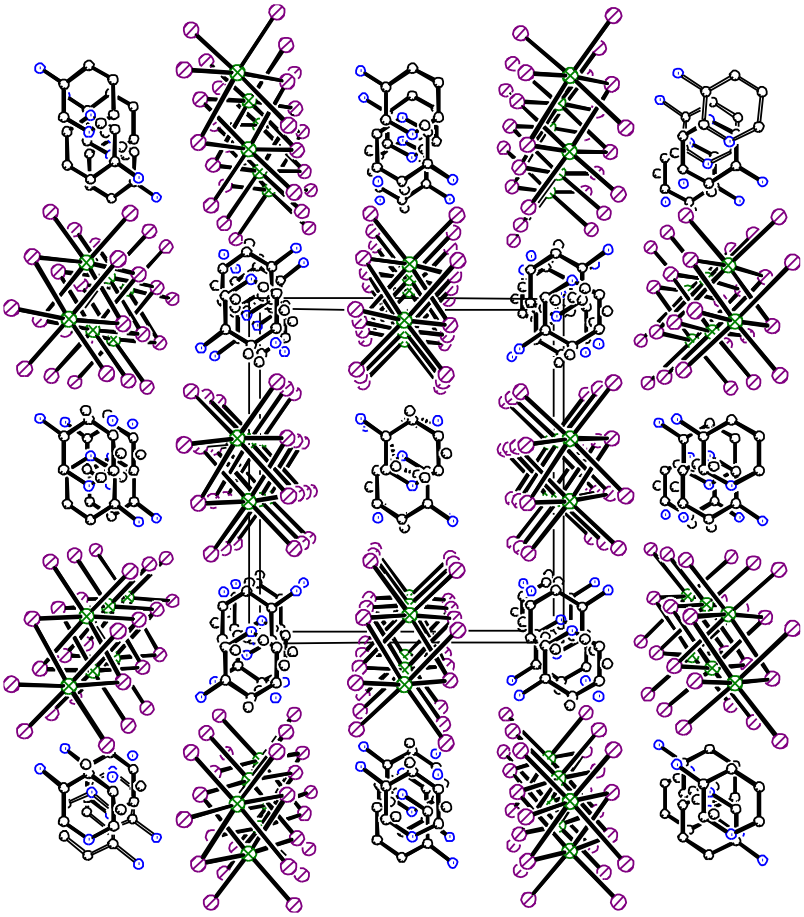

Figure S4 Projection of the structure of **2** along the *a* axis.

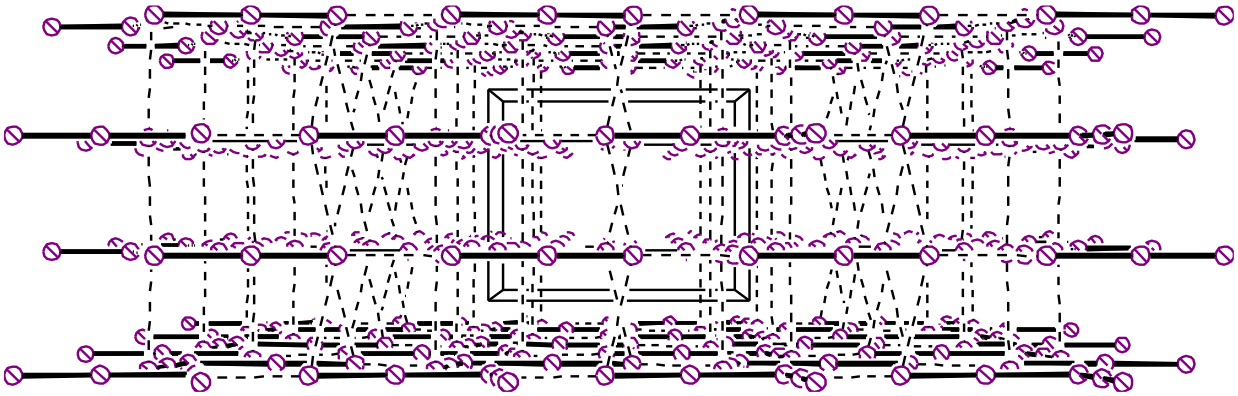

(*a*)

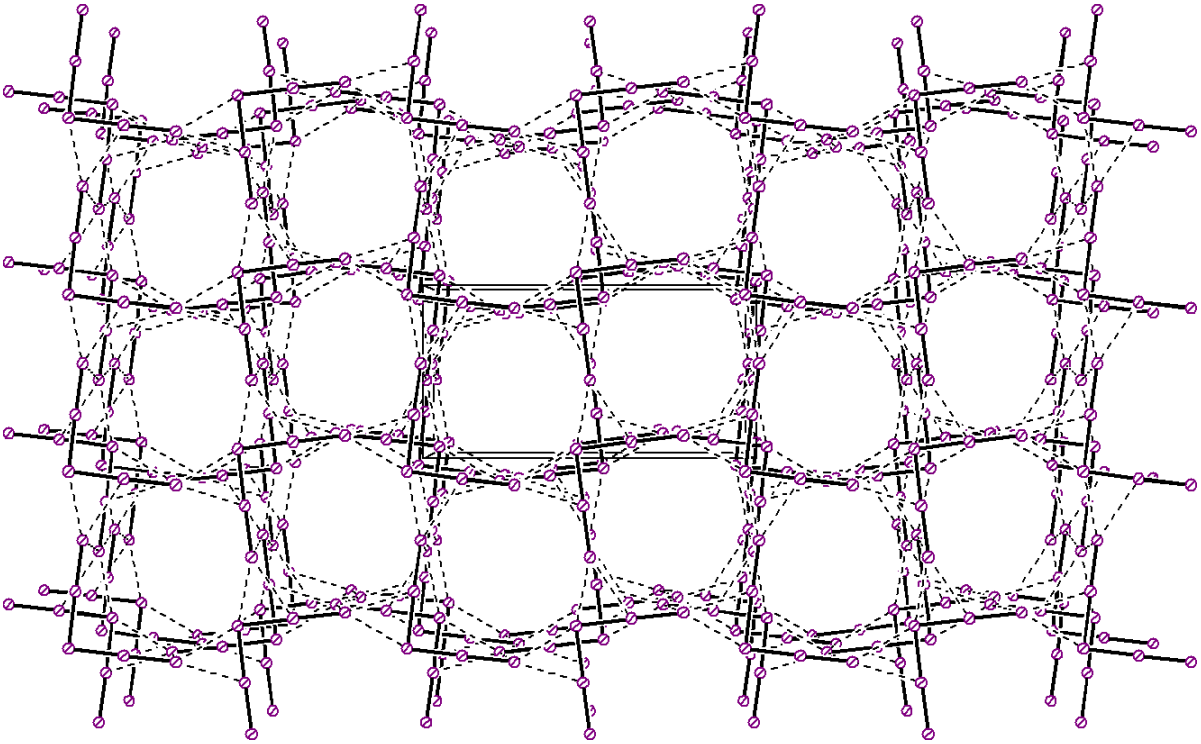

(*b*)

Figure S5 Projections of the anion sublattice of **4** along (*a*) the *b* (*b*) and *c* axes. Contacts shorter than 4.1 Å are indicated by dashed lines.

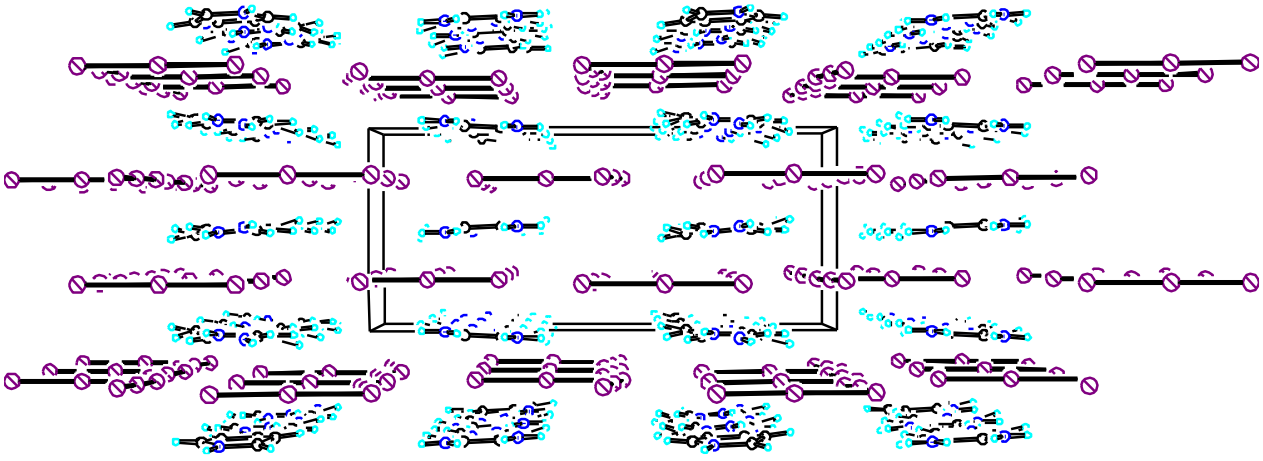

(*a*)

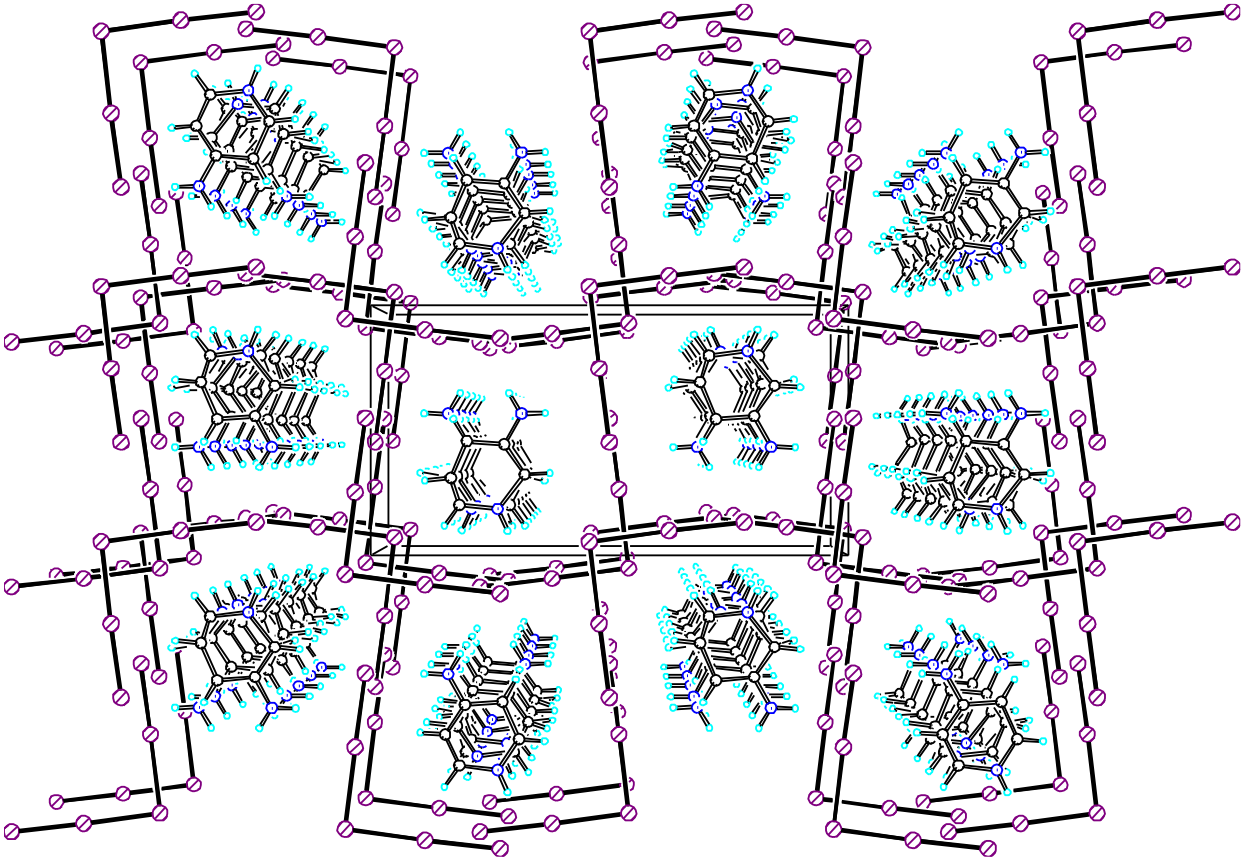

(*b*)

Figure S6 Projections of the structure of **4** along (*a*) the *b* (*b*) and *c* axes.

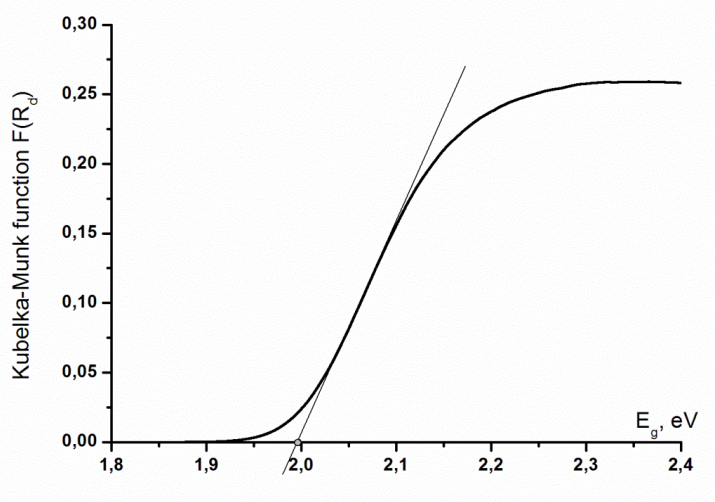

(*a*)

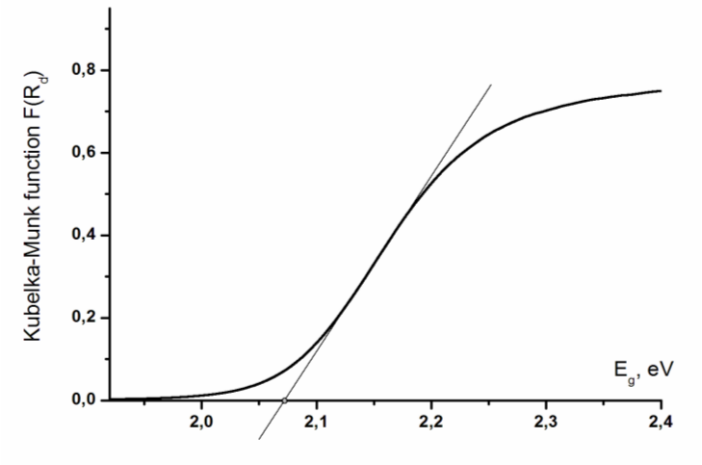

(*b*)

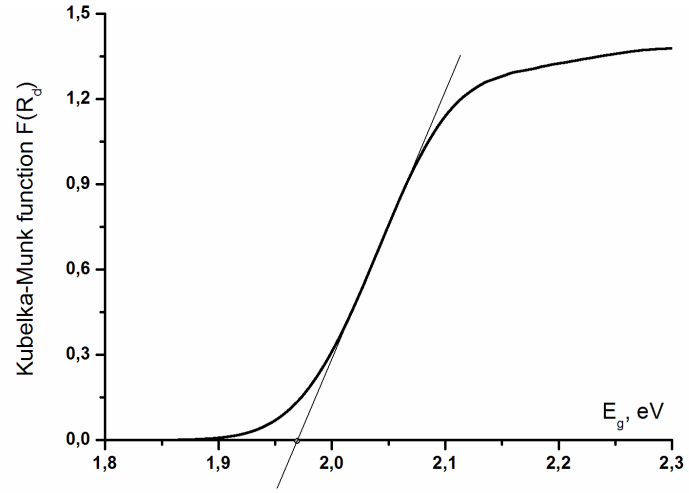

(*c*)

Figure S7 Reflectance spectra of (*a*) **1**, (*b*) **2**, (*c*) and **3**.

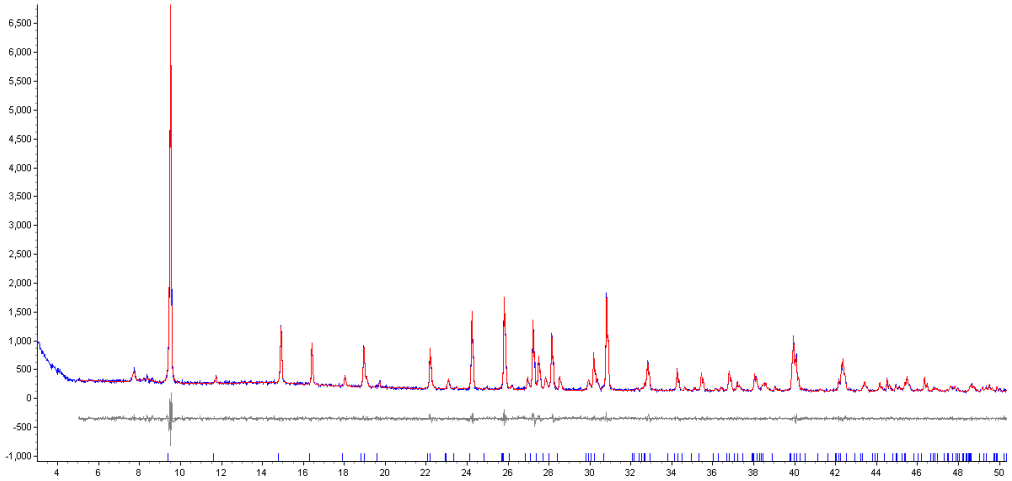

(*a*)

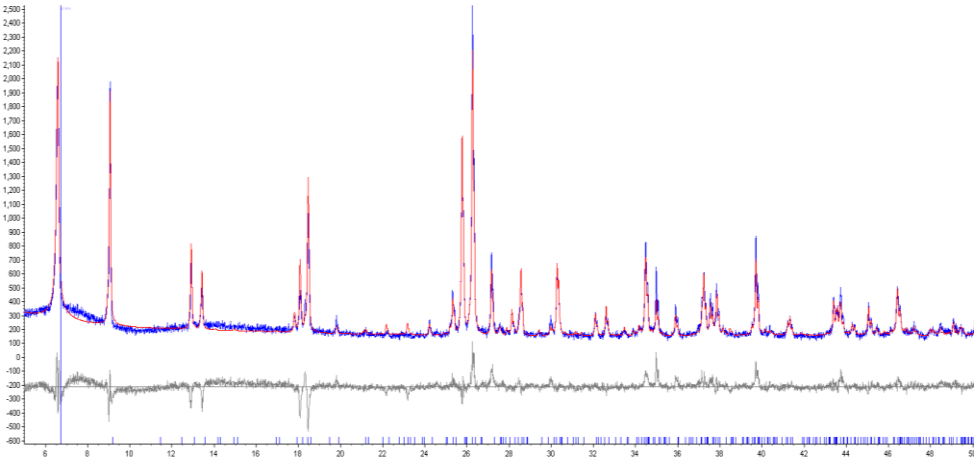

(*b*)

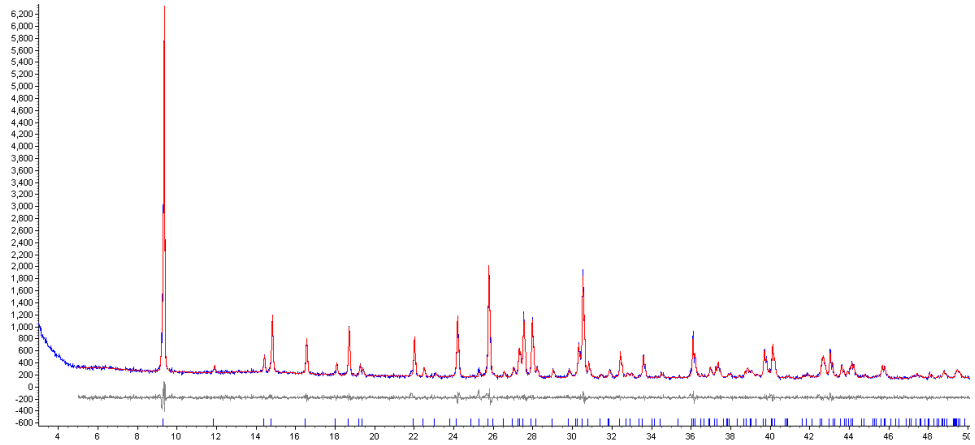

(*c*)

Figure S8 X-ray Rietveld refinement profiles for (*a*) **1**, (*b*) **2**, (*c*) and **3** recorded at room temperature. Red and blue lines correspond to the calculated profile and experimental pattern, respectively. The bottom trace shows the difference curve. The vertical bars indicate the calculated positions of the Bragg peaks.

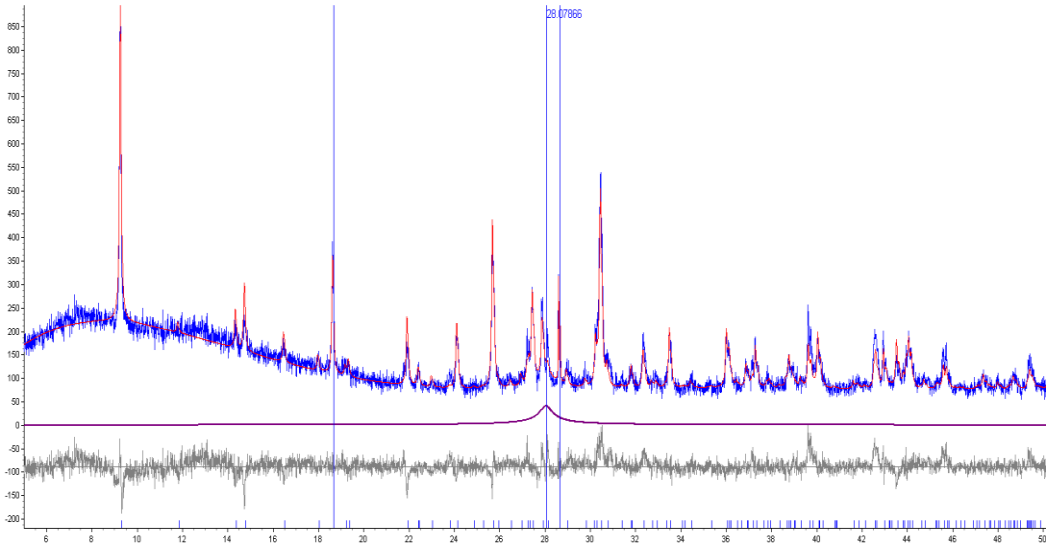

Figure S9 X-ray Rietveld refinement profiles for **3** after its dissolution in concentrated HI and subsequent crystallization in air atmosphere at room temperature. Red and blue lines correspond to the calculated profile and experimental pattern, respectively. The bottom trace shows the difference curve. The vertical bars indicate the calculated positions of the Bragg peaks.